Vol. 18, No. 3 (2019) 803-812
Revista Mexicana de Ingeniería Química

MODELLING OF CONTINUOUS PRODUCTION OF BIOGAS IN A TUBULAR REACTOR

MODELADO DE LA PRODUCCIÓN CONTINUA DE BIOGÁS EN UN REACTOR TUBULAR

M. Romero-Flores[1]*, M.V. Sillas-Moreno[1], E. Trejo[2], A. Montesinos-Castellanos[1]

[1]*Tecnológico de Monterrey, Escuela de Ingeniería y Ciencias. Eugenio Garza Sada 2501 Sur, C.P. 64849, Monterrey, N.L., México.*

[2]*TERNIUM. Av. Guerrero Nte. No. 151 Col. Cuauhtémoc, San Nicolás de los Garza, Monterrey, N.L. C.P. 66437, México*

Received: July 23, 2018; Accepted: October 19, 2018

Abstract

In this work a new model was developed, simulated and compared experimentally for the prediction of biogas production in a tubular reactor. The model presented here consider cell degradation in a tubular reactor. To test and validate this model, a prototype was built and tested. The simulation of fluid dynamics and concentration gradients was carried out in a one-dimensional system using finite elements, and, according to the results of these simulations, the production of biogas in the tubular reactor was divided into different strata. This may be due to the diffusion of the substrate through the reactor, which causes different growth rates for microorganisms which depend on the availability of the substrate. Theoretical and experimental results showed good agreement with each other. The results obtained in this work can support the understanding of the bacteria decay in small bioreactors and therefore, helping in the development of a compact, simple and efficient system capable of produce continuously biogas on a small scale.

Keywords: biogas, tubular reactor, renewable energy, biomass, CFD.

Resumen

En este trabajo se desarrolló, simuló y comparó experimentalmente un nuevo modelo para la predicción de la producción de biogás en un reactor tubular. El modelo aquí presentado es un modelo que considera la degradación celular dentro de un reactor tubular. Para probar y validar este modelo, se construyó y probó un prototipo de reactor tubular. La simulación de la dinámica de fluidos y los gradientes de concentración se llevó acabo en un sistema unidimensional utilizando elementos finitos y, de acuerdo con los resultados, la producción de biogás dentro del reactor tubular se divide en diferentes estratos. Esto puede deberse a la difusión del sustrato a través del reactor, lo cual provoca un crecimiento distinto de microorganismos según la disponibilidad del sustrato. Los resultados teóricos y experimentales mostraron una buena concordancia entre sí. Los resultados obtenidos en este trabajo pueden ayudar en la comprensión del decaimiento de bacterias en biorreactores pequeños, ayudando en el desarrollo de un sistema compacto, simple y eficiente capaz de producir biogás a baja escala de manera continua.

Palabras clave: biogás, reactor tubular, energía renovable, biomasa, CFD.

1 Introduction

Since the Industrial Revolution at the beginning of the XIX century, energy demand has been increasing. Most of the energy that we use comes from fossil fuels, which will disappear within this century if the ascending energy demand remains. Additionally, the exploitation of fossil fuels has caused environmental disequilibrium and pollution in all ecosystems; one consequence of this is global warming, generated mainly by CO_2 emissions produced in combustion processes.

In response to the current global energy use scenario, recent investigations have focused on the development and utilization of renewable energy sources and the improvement of usage efficiency (Painuly, 2001; Orozco-Hernández *et al*., 2016; Destek and Aslan, 2017; Brini *et al*., 2017). One of these resources is biomass, the use of which as an energy source has been applied in a variety of ways (McKendry, 2002; Ortíz-Méndez, *et al*., 2017;

* *Corresponding author. E-mail*: michel308@gmail.com
https://doi.org/10.24275/uam/izt/dcbi/revmexingquim/2019v18n3/Romero
issn-e: 2395-8472

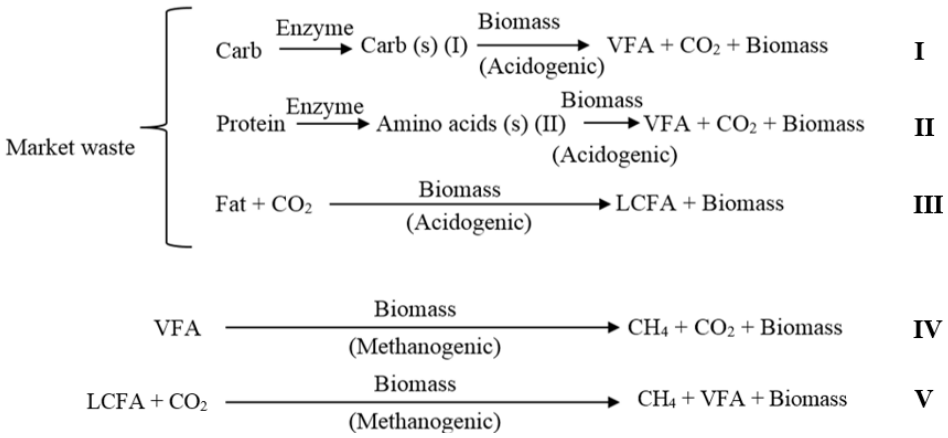

Fig. 1. Mechanism proposed by Biswas *et al*. (2006) for anaerobic digestion.

Proskurina *et al*., 2017; Sanchez-Herrera *et al*., 2018). One option for using biomass as an energy source is the production of methane by anaerobic digestion of biodegradable organic materials. Biogas is produced in closed reactors in the absence of dissolved oxygen. Most of the current plants that produce biogas use the organic part of municipal solid wastes as raw material. Processes vary according to substrate characteristics and quantity to be treated. This technology has proven to be economically feasible on a large scale. However, the low-scale systems that have been developed to this point cannot compete in efficiency and operation costs with large-scale plants.

The main challenge in the operation of small-scale systems is the change in the type and amount of biomass fed into the system. When amounts greater than those that can be processed are supplied to the population of bacteria, this inhibits methanogenic activity, which can permanently affect the process of the production of methane. The traditional way to produce biogas in controlled conditions is with continuous stirred-tank reactors (CSTRs), where the feed comes in contact instantly with the entire population of bacteria. This procedure has certain disadvantages, since a rapid generation of acid may have significant effects on the methanogenic colony. Methanization is achieved through a mixture of microorganisms and is composed of different stages.

The anaerobic digestion process is very complex from a kinetic point of view, since many reactions are involved (Zuru *et al*., 2004). Different kinetic models have been proposed, and most of them use chemical oxygen demand (COD) to express substrate concentration during the process, while biomass concentration is expressed by the amount of suspended solids.

The kinetic models most commonly used to describe the kinetics of anaerobic digestion processes have been the Monod type (Anderson *et al*., 1996), which considers that the growth rate of bacteria is a function of substrate concentration and bacteria population. The most significant feature of this model is that the production rate is zero when there are no bacteria or substrate and that it rate tends to a maximum limit when the substrate is in excess (Lobry *et al*., 1992). Different modifications have been applied to the Monod model to increase its accuracy in different scenarios (Nicoletta *et al*., 2014). For example, Biswas *et al*. (2006) and Zuru *et al*. (2004) used the volume fraction of biogas as a concentration variable for the application of a kinetic model. Other models have been developed and studied with interesting results (Nicoletta *et al*., 2014; Akbas *et al*., 2015; Chatterjee *et al*., 2017)

One of the models based on that of Monod is proposed by Biswas *et al*. (2006), who conducted studies to determine the kinetics of biogas production from municipal wastes. In their experiments, they used three different substrates that were characterized to determine the percentage of carbohydrates, proteins, and fats. These three substrates were considered separately, and their use was dependent on different types of bacterial colonies.

To establish their kinetic model, Biswas *et al*. (2006) proposed the mechanism shown in Fig. 1. In Fig. 1, it can be seen that soluble carbohydrates and

amino acids are formed through enzymatic hydrolysis, while the volatile acids and long chain acids are formed by acidogenic degradation. In equations shown in Fig. 1, volatile fatty acids (VFAs), and long-chain fatty acids (LCFAs) are formed in the acidogenic process used by the colony of methanogenic bacteria (MB) to produce biogas. Biswas *et al*. (2006) considered that the solubilization stage is much faster than the other phases involved in the anaerobic fermentation process; therefore, in this model, the formation of soluble carbohydrates and amino acids is considered to be instantaneous.

As mentioned above, the Monod model was used in the biological reaction equations. Biswas *et al*. (2006) used a modified Monod model [Eq. (1)] for the prediction of cell growth in different parts of the reaction process:

$$r_i = \frac{\mu_{\max i} c_{bi} c_{Si}}{K_{Si} + c_{Si}} \tag{1}$$

To determine the parameters of the model (Table 1), Biswas *et al*. (2006) performed experiments in which they separated acidogenic bacteria (AB) and methanogenic bacteria.

Due to the great similarity between the experimental data and those obtained by the model proposed by Biswas *et al*. (2006), and taking into account that the composition in terms of percentages of carbohydrates, proteins, and fats for the substrate is more common than elemental analysis or COD (parameters used in other kinetic models), we used this model as a basis for simulating the operation of anaerobic digestion in a tubular reactor.

To understand some of the difficulties in the biogas production process and to improve its performance, simulations of the degradation process using a kinetic model may be done. These simulations have great benefits, as they allow an overview of the system operation at low cost. Additionally, there are no risks in the real process, for no physical modifications are needed. Other authors have shown on their works the benefits of simulations for the design and optimization of bioreactors and other kind of equipment. (Haringa *et al*., 2018; Kang *et al*., 2013; Trejo *et al*., 2012; Moilanen *et al*., 2006)

In this study, the kinetic model developed by Biswas *et al*. (2006) was applied to a tubular reactor using an intermittent feeding method. Additionally, a modification to the original model was proposed to include inhibition of methane production caused by high concentrations of acids in the reactor. Finally, the simulation results will be compared with experimental results.

2 Proposed modeling and simulation

2.1 *Kinetic model*

The equations proposed by Biswas *et al*. (2006) do not consider the decay of the bacteria population; as a result, it is necessary to modify their model to include this phenomenon.

Liu *et al*. (2008) developed a kinetic model for anaerobic digestion that uses a mortality factor proportional to the concentration of the bacteria. Mortality constants used in the model were calculated by Kiely *et al*. (1997) for methanogenic bacteria and Moletta *et al*. (1986) for acidogenic bacteria. The values of these constants are 0.06 d^{-1} and 0.016 d^{-1} for acidogenic and methanogenic bacteria, respectively.

Table 1. Kinetic parameters estimated by Biswas *et al*. (2006).

Reaction	Kinetic parameters		Y (yield coefficients)						
Parameter	$\mu_{\max}$	K_S	*car*	*pro*	*fat*	*LCFA*	*VFA*	CO_2	CH_4
Carbohydrates: acidogenesis	5.17	0.518	13.15				9.95	2.412	
Proteins: acidogenesis	6.4	0.2		14.49			12.21	1.733	
Fat: acidogenesis	0.55	0.1			181.8	184		1.26	
VFA: methanogenesis	2.44	0.049					20.83	11.13	9.522
LCFA: methanogenesis	0.559	0.019				9.8	18.2	6.289	1.905

To account for the inhibition of methane production and the decrease in the activity of acidogenic bacteria in the presence of high concentrations of acid, the present study proposed a variable mortality factor, which depends on the acid concentration in the reactor:

$$K_{da} = 0.06 + \varepsilon_1 (c_{VFA} + c_{LCFA}) \quad (2)$$

$$K_{dm} = 0.016 + \varepsilon_2 (c_{VFA} + c_{LCFA}) \quad (3)$$

A least square adjustment to the experimental data for the production of methane was performed to determine the values of the constants ε_1 and ε_2. The obtained values were 0.2 L g^{-1} d^{-1} and 4 L g^{-1} d^{-1}, respectively.

Applying the mortality factors in the equations obtained by Biswas *et al*. (2006), we obtained the final equations for cell growth (Table 2).

In Table 2, equations 4-8 describes the biomass formation rate of Fig. 1 reactions. Equations 9-15 describes the reaction rate for all the other components of the reactions (Carbohydrates, protein, fat, VFA, LCFA, CO_2 and CH_4).

For equations of Table 2 irreversible reactions at constant T (37 ºC) and P (1 atm) were considered.

Table 2. Proposed model for the simulation.

$$r_{b_I} = \frac{\mu_{\max_{car}} c_{b_a} c_{S_{car}}}{K_{S_{car}} + c_{S_{car}}} - K_{da} c_{b_a} \quad (4)$$

$$r_{b_{II}} = \frac{\mu_{\max_{pro}} c_{b_a} c_{S_{pro}}}{K_{S_{pro}} + c_{S_{pro}}} - K_{da} c_{b_a} \quad (5)$$

$$r_{b_{III}} = \frac{\mu_{\max_{fat}} c_{b_a} c_{S_{fat}}}{K_{S_{fat}} + c_{S_{fat}}} - K_{da} c_{b_a} \quad (6)$$

$$r_{b_{IV}} = \frac{\mu_{\max_{VFA}} c_{b_m} c_{S_{VFA}}}{K_{S_{VFA}} + c_{S_{VFA}}} - K_{dm} c_{b_m} \quad (7)$$

$$r_{b_V} = \frac{\mu_{\max_{LCFA}} c_{b_m} c_{S_{VFA}}}{K_{S_{LCFA}} + c_{S_{LCFA}}} - K_{dm} c_{b_m} \quad (8)$$

$$r_{car} = -Y_{car \to VFA} r_{b_I} \quad (9)$$

$$r_{pro} = -Y_{pro \to VFA} r_{b_{II}} \quad (10)$$

$$r_{fat} = -Y_{fat \to LCFA} r_{b_{III}} \quad (11)$$

$$r_{LCFA} = Y_{fat \to LCFA} r_{b_{III}} - Y_{LCFA \to CH_4} r_{b_V} \quad (12)$$

$$r_{VFA} = Y_{car \to VFA} r_{b_I} + Y_{pro \to VFA} r_{b_{II}} - Y_{VFA \to CH_4} r_{b_{IV}} + Y_{LCFA \to VFA} r_{b_V} \quad (13)$$

$$r_{CO_2} = Y_{car \to CO_2} r_{b_I} + Y_{pro \to CO_2} r_{b_{II}} - Y_{CO_2 \to LCFA} r_{b_{III}} + Y_{VFA \to CO_2} r_{b_{IV}} - Y_{CO_2 \to CH_4} r_{b_V} \quad (14)$$

$$r_{CH_4} = Y_{VFA \to CH_4} r_{b_{IV}} + Y_{LCFA \to CH_4} r_{b_V} \quad (15)$$

To determine the behavior of the substrates, intermediates, and final products within the tubular reactor, the conservation equation of chemical species, Eq. (16), was resolved on a one-dimensional domain:

$$\frac{\partial \rho_A}{\partial t} + \mathbf{v} \cdot \nabla \rho_A = \mathscr{D}_{AB} \nabla^2 \rho_A + r_A \quad (16)$$

2.2 Setting subdomain properties and boundary conditions

The proposed system of equations was solved using the finite element COMSOL Multiphysics® software (COMSOL, Inc., Burlington, MA, USA). A tubular reactor with the same dimensions and temperature as the real reactor (see section 3) was simulated. Operation was simulated in a transient state. The simulated feed was 25 ml/d to obtain a hydraulic residence time of 340 d. The substrate was instantly

fed into the reactor at the beginning of each day of simulation.

2.2.1 *Initial conditions*

The concentration of primary and secondary substrate and fermentation products was considered zero at the beginning, for an empty reactor was considered. For the population of bacteria, concentration of 0.001 g/L for groups of acidogenic bacteria and 0.002 g/L for groups of methanogenic bacteria were used for similar conditions and inoculums, as reported previously by Biswas *et al*. (2006). The concentration of fat, protein and carbohydrates used, were the same as in the experiment (see section 3).

2.2.2 *Boundary conditions*

To simulate a similar condition to the experimental in the feed, a periodic function, which provides a flux of substrates in a pulse shape at the entrance of the tubular reactor for each day of simulation, was used. The flow rate was estimated with the volume of the feed and was activated by the periodic function used for feeding substrates. In the reactor outlet, a convective flux condition was set for the substrates, bacteria and gases. Also, for the gases, an inlet wall condition was used, this to simulate the same conditions as in the experiment.

2.2.3 *Subdomain*

The equations were solved in a one-dimensional time-dependent system because the concentrations did not have significant variation in the radial and angular coordinates of the reactor. This may be caused by the slow axial flow in the reactor. The dimensional subdomain used for the simulation consisted of 300 elements distributed along the reactor, using smaller element separation in the inlet and outlet as follows: From 0 to 0.15 m 50 elements were used, from 0.15 to 1.55 m 200 elements were used and from 1.55 to 1.7 m 50 elements were used. This amount and distribution of elements was used, for no significant variation in the results was observed when a higher number was used.

3 Experimental setup

On Biswas *et al*. (2006) work, experiments were done using a bioreactor of V=10 L. For bigger systems the effect of the bacteria decay may not be significant. Therefore, to observe this effect, a smaller bioreactor was built in this work (V=3.4 L).

The system was similar to a double pipe heat exchanger. It was composed by two PVC pipes, the inner pipe (digestion chamber, Fig 2A) with D_i=0.0508 m (2 in) and L= 1.7m (67 in) and the outer pipe (heating jacket, Fig. 2B) with D_i=0.0762 m (3 in) and with the same length as the digestion chamber. The external pipe (heating jacket) had a thermal insulator (Fig. 2C) to reduce heat losses. The digestion chamber includes an inlet for the biomass (Fig. 2D), an outlet for the liquid waste (Fig. 2E) and an outlet for the biogas produced (Fig. 2F).

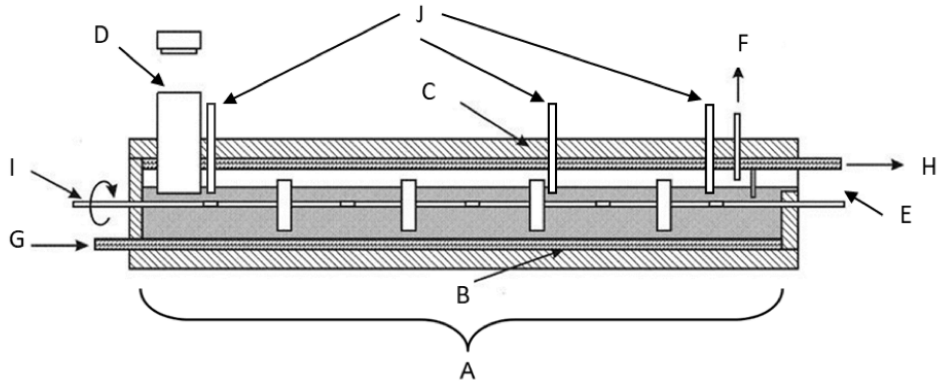

Fig. 2. Bioreactor components. (A) Digestion chamber. (B) Heating jacket. (C) Thermal insulator. (D) Biomass inlet. (E) Liquid waste outlet. (F) Biogas outlet. (G, H) Heating water inlet and outlet. (I) Concentric agitator and propellers. (J) pH measurement points.

Similarly, the heating jacket includes an inlet and outlet for the water used as heating fluid flowing through the annular space (Fig. 2G and H respectively). Inside the digestion chamber, there was a concentric agitator (Fig. 2I) built with acrylic and powered by an electric motor to 20 RPM. Additionally, the digestion chamber had three pH measurement points at 0, 1 and 1.5m (Fig. 2J). These lengths were selected because significant information was obtained using these points. The biomass (the grey zone inside the digestion chamber in Fig. 2) occupied three-quarters of the volume of the digestion chamber (total volume of the digestion chamber = 3.4 L), keeping the upper part free for the accumulation of the biogas produced (The white zone inside the digestion chamber in Fig. 2). This bioreactor was designed to produce biogas continuously, using a semi batch feed for the biomass.

More details regarding the design of the bioreactor can be found in Montesinos-Castellanos and Trejo-Treviño (2018) work.

The reactor was loaded with 2.5 L of inoculum, and it was fed with a 25 ml solution containing 3 g of biomass for 25 d in 12 hours intervals. Fat, protein and carbohydrate concentrations in the biomass were: 0.336 g/L, 2.9 g/L and 8.62 g/L respectively.

Biogas production began on the third day and increased to reach a stable value, in which, both the amount of biogas produced, and its composition remained constant. The temperature inside the reactor was maintained under mesophilic conditions (37 °C). The pH was measured daily during the first two weeks of operation. Afterwards, when no significant variations in pH were observed, measurements were taken once a week. The experiment was replied five times.

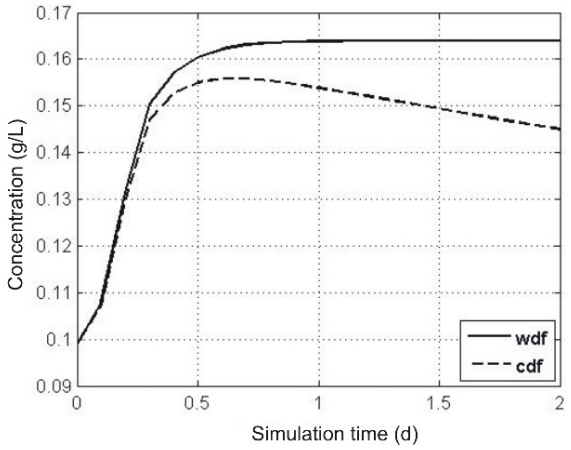

Fig. 3. Population of bacteria without decay factor (wdf) and with constant decay factor (cdf).

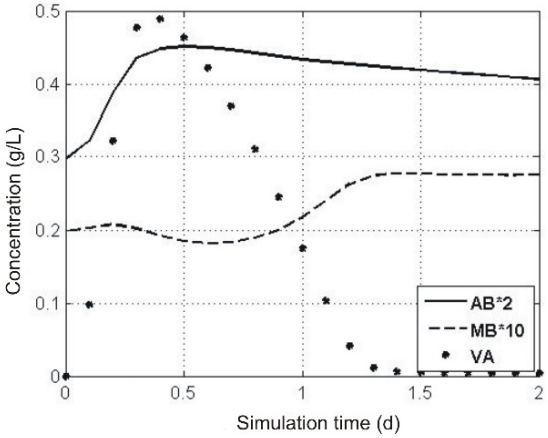

Fig. 4. Concentration behavior of acidogenic bacteria (AB), methanogenic bacteria (MB), and volatile acids (VFA) when a variable decay factor is added to the model.

In the model of Biswas *et al*. (2006), after feeding the substrate, the bacteria showed an exponential growth in the first stage. However, when decreasing the concentration of the substrate, the growth rate decreases consistently until the substrate is consumed. Moreover, when the substrate is totally consumed, the bacterial population reaches a maximum and remains constant for the rest of the simulation. In the proposed model, bacteria also have an exponential growth in the first moments until reaching maximum concentration, but, after this stage, the concentration of bacteria begins to decline because of natural decay in the absence of the substrate. Another reason for the overestimated methane production predicted by Biswas *et al*. (2006) is that bacteria are not affected by the high concentrations of acids produced, and they can continue metabolizing substrate without being affected by this factor. In the case of the proposed model, a mortality rate that varies with the concentration of acids present has been included. Thus, with this modification, closer results to previous experiments may be obtained, where high concentrations of acids inhibit methanogenic activity. Fig. 4 shows the behavior in the concentration of bacteria that results from adding the variable mortality factor (Eqs. 2 and 3) to the corresponding Monod equations.

By replacing the constant mortality factor for a variable factor, it is possible to simulate the inhibition caused by the increase in acid concentration. Fig. 4 shows an exponential growth of acidogenic and methanogenic bacteria at the start of the process.

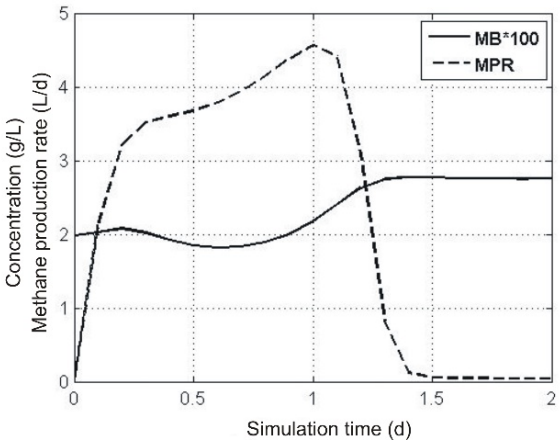

Fig. 5. Variation of methanogenic bacteria (MB) population and its impact on methane production rate (MPR) when the variable decay factor is added to the model.

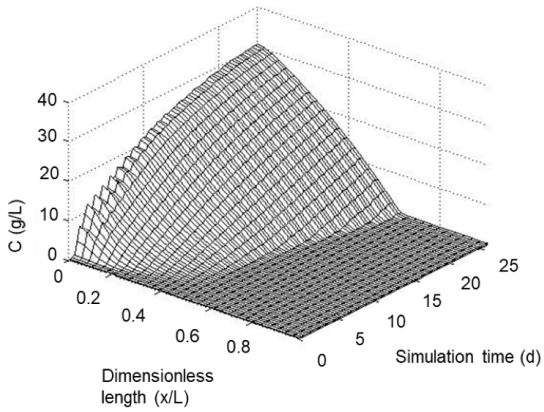

Fig. 6. Acid concentration distribution (VFAs and LCFAs in g/L) along the reactor thought time; dimensionless length was used.

This generates high concentrations of acid, reverting the rising trend of methanogenic bacteria, which is reflected in a decrease in methane production (Fig. 5). This simulation results were correlated with the experimental data with good agreement.

3.1 Semi-batch simulation for the tubular reactor

In the simulation carried out for the tubular reactor, the production maintained a rising trend in the succeeding days and did not show any inhibition. The population of acidogenic bacteria in the reactor inlet increased significantly during the first days to levels of 1.2 g/L, while the population of methanogenic bacteria remained low in the same region due to the generation of acids by the acidogenic bacteria.

The diffusion of acids produced allowed the population of methanogenic bacteria to begin to grow significantly to about 20 cm from the reactor inlet from the third day of simulation, whereas the dilution of the acids allowed conditions for metabolism and reproduction. The acidogenic bacteria population decreased sharply with the increasing distance from the entrance to the reactor, which was caused by the diffusion of the same and lower substrate through the reactor.

Fig. 6 shows the variation of the VFAs and LCFAs concentration produced by the acidogenic bacteria through the reactor, for a simulation time of 25 days. According to this figure, acids showed concentration variations in the first 60% of the reactor section for a simulations time of 25 days. The acids concentration increased first in the inlet, and then, through the reactor the next days. A maximum concentration of ~32% was observed in the inlet for 25th day. This behavior could be explained by two mechanisms. First, the acids move through the system by diffusion and then, methanogenic bacteria consumes them, retarding their movement through the reactor.

High acid concentrations inhibit the development of methanogenic bacteria. However, the acid is also essential for the metabolism of these bacteria. For this reason, we can see that the concentration of methanogenic bacteria decreased in high concentrations of acid, but also decreased in their absence (Fig. 7). The periodic behavior of the concentration of different substances involved in the proposed model for anaerobic digestion shows the steady-state reactor condition.

The simulation shows a clear separation between the two groups of bacteria involved in the model. The acidogenic bacteria proliferate in the first section of the reactor where the primary substrates exist in sufficient concentration, and the methanogenic bacteria grow where the inhibitory effect of acids is reduced by diffusion.

As can be observed in the results obtained, there was a significant difference when using the proposed model compared to that of Biswas *et al*. (2006). However, there is a need for experimental data to determine the accuracy of our model. This will be discussed in the next section.

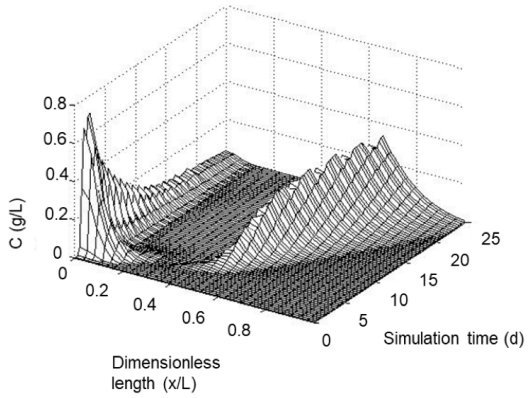

Fig. 7. Distribution over time of acidogenic bacteria concentration in the tubular reactor system; dimensionless length was used.

3.2 Comparison with experimental data

The distribution shown in Fig. 7 is supported by the experiments were the pH data measured in the tubular reactor at different lengths, were 6, 7.8, and 7.9 for distances of 0, 1, and 1.5 m, respectively.

The values of the daily accumulated methane production that were experimentally observed were similar to those projected by the proposed model in this study, as shown in Fig. 8. In this case, there were no significant differences at the beginning of the operation, since the limiting factors for the utilization of the substrates were not diffusivity and solubility; therefore, although the model substrates were available in an instant, these were only consumed when they were in contact by diffusion with the bacteria.

Upon reaching a constant biogas production, approximately after day 10 as observed in Fig. 8, the values of the simulation and the experimental data showed a strong agreement, with methane yields of 0.45 L/d, which indicated that the model chosen to describe the kinetics of the reaction was accurate, at least in terms of methane production according to the conditions under which the experiment was conducted. However, to determine the correlation of other substances involved, it would be necessary to take samples at different reactor lengths and compare them with those projected by the model. For instance, different measurements of the acids (VFAs and LCFAs) could be done to compare them with the model results. Moreover, according to the results of the simulation shown in Fig. 6, it would be preferable to measure the acids in the first 60% of the reactor section

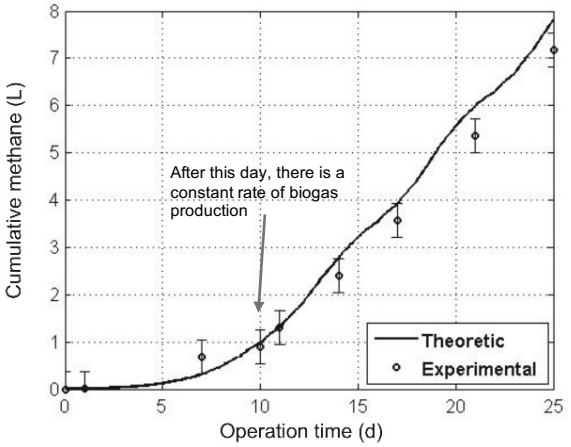

Fig. 8. Comparison of the experimental production of methane and simulation results for the tubular reactor. The arrow indicates where the constant production rate of biogas begins.

for 25 days to obtain comparable data. Furthermore, using enough measurement points is essential to obtain a good comparison.

Conclusions

With the proposed model, a better estimation of the degradation process may be obtained, even when there are considerable variations in the concentration of species across the operation time. Also, it can model the behavior of the reactor when the supply frequency or its quantity is modified.

The addition of a variable decay factor to the model allowed a better agreement between simulations and the experimental data. Two coefficients have been estimated to account for the inhibition of acidogenic and methanogenic bacteria when fatty acids are present. At the same time, this factor predicts different growth rates for bacteria groups across the tubular reactor, which is a desirable condition in actual biogas production systems. However, more systematic studies are needed to validate the model proposed here.

Using the developed model, it is possible to identify the bacteria decay in small bioreactors. Thus, to help in the design of a reactor that is efficient in association with the organic material available. Also, these results could help to do changes to the previously installed systems.

Acknowledgements

The support provided by the Instituto Tecnológico de Estudios Superiores de Monterrey and Nutec Bickley for the development of this investigation is gratefully appreciated. This research is a product of the Project 266632 "Laboratorio Binacional para la Gestión Inteligente de la Sustentabilidad Energética y la Formación Tecnolo?gica" ("Bi-National Laboratory on Smart Sustainable Energy Management and Technology Training), funded by the CONACYT SENER Fund for Energy Sustainability (Agreement: S0019-2014-01).

Nomenclature

c_{Si}	substrate concentration of species i, g L^{-1}
c_{ba}	biomass concentration of acidogenic reactions, g L^{-1}
c_{bm}	biomass concentration of methanogenic reactions, g L^{-1}
D_i	internal diameter, m
$\mathscr{D}_{AB}$	diffusion coefficient, m^2 s^{-1}
i	subscript used to define the specie, it can be: car (carbohydrates), pro (protein), fat, CO_2, VFA (Volatile Fatty Acids), LCFA (Long-Chain Fatty Acids) or CH_4 (Methane)
k	subscript used to define the biomass reaction number, it goes from I to V
K_{Si}	saturation constant of substance i, g L^{-1}
K_{da}	mortality factor of acidogenesis, d^{-1}
K_{dm}	mortality factor of methanogenesis, d^{-1}
L	length, m
r_{bk}	reaction rate of biomass reaction k, mol L^{-1} d^{-1}
r_i	reaction rate of substance i, mol L^{-1} d^{-1}
v	velocity, m s^{-1}
V	volume of the system, L
$Y_{i\rightarrow j}$	yield coefficient for i substance to j product, ([g of i produced] [g of biomass produced^{-1}])
Greek symbols	
$\mu_{\max i}$	maximum specific growth rate of microorganisms for reaction of substance i,d^{-1}
ε_1	constant for K_{da} determination, L g^{-1} d^{-1}
ε_2	constant for K_{dm} determination, L g^{-1} d^{-1}
ρ_A	density of component A, Kg m^{-3}

References

Anderson, G.K., Kasapgil, B. and Ince, O. (1996). Microbial kinetics of a membrane anaerobic reactor system. *Environmental Technology 17*, 449-464.

Akbaş, H., Bilgen, B. and Turhana, A. M. (2015). An integrated prediction and optimization model of biogas production system at a wastewater treatment facility. *Bioresource Technology 196*, 566-576.

Biswas, J., Chowdhury, R. and P. Bhattacharya (2006). Kinetic studies of biogas generation using municipal waste as feed stock. *Enzyme and Microbial Technology 38*, 493-503.

Brinia, R., Amarab, M. and Jemmalic, H. (2017). Renewable energy consumption, International trade, oil price and economic growth inter-linkages: The case of Tunisia. *Renewable and Sustainable Energy Reviews 76*, 620-627.

Chatterjee, P., Ghangrekar, M. M. and Rao, S. (2017). Biogas production from partially digested septic tank sludge and its kinetics. *Waste and Biomass Valorization 8*, 1-12.

Desteka, M.A. and Aslan, A. (2017). Renewable and non-renewable energy consumption and economic growth in emerging economies: Evidence from bootstrap panel causality. *Renewable Energy 111*, 757-763.

Haringa, C., Tang, W., Wang, G., Deshmukh, A.T., van Winden, W.A., Chu, J., van Gulik, W.M., Heijnen, J.J., Mudde, R.F. and Noorman, H.J. (2018). Computational fluid dynamics simulation of an industrial *P. chrysogenum* fermentation with a coupled 9-pool metabolic model: Towards rational scale-down and design optimization. *Chemical Engineering Science 175*, 12-24.

Kang, C., Wang, Y., Tania, M., Zhou, H., Gao, Y., Ba, T., Tan, G.S., Kim, S. and Leo, H.L. (2013). Computational fluid modeling and performance analysis of a bidirectional rotating perfusion culture system. *Biotechnology Progress 29*, 1002-1012

Kiely, G., Tayfur, G., Dolan, C. and Tanji, K. (1997). Physical and mathematical modelling

of anaerobic digestion of organic wastes. *Water Research 31*, 534-540.

Kythreotou, N., Florides, G. and Tassou, S. A. (2014). A review of simple to scientific models for anaerobic digestion. *Renewable Energy 71*, 701-714.

Liu, C.F., Xing-zhong, Y., Guang-ming, Z., Wen-wei, L. and Jing, L. (2008). Prediction of methane yield at optimum pH for anaerobic digestion of organic fraction of municipal solid waste. *Bioresource Technology 99*, 882-888.

Lobry, J., Flandrois, J.P., Carret, G. and Pave, A. (1992). Monod's bacterial growth model revisited. *Bulletin of Mathematical Biology 54*, 117-122.

McKendry, P. (2002). Energy production from biomass (part 1): Overview of biomass. *Bioresource Technology 83*, 37-46.

Moilanen, P., Laakkonen, M. and Aittamaa, J. (2006). Modeling aerated fermenters with computational fluid dynamics. *Industrial & Engineering Chemistry Research 45*, 8656-8663.

Moletta, R., Verrier, D. and Albagnac, G. (1986). Dynamic modelling of anaerobic digestion. *Water Research 20*, 427-434.

Montesinos-Castellanos, A. and Trejo-Treviño, E. (2018). Reactor tubular para la producción de metano a partir de la digestión anaerobia de materia. Monterrey, Nuevo León, 64849, MX. Patent No. 354107.

Orozco-Hernández, J.M., Romero, R., Natividad, R., and Baeza-Jiménez, R. (2016). Improvement strategies for the enzymatic production of biodiesel in the presence of primary alcohols. *Revista Mexicana de Ingeniería Química 15*, 935-942.

Ortíz-Méndez, O.H., Morales-Martínez, T.K., Rios-González, L.J., Rodríguez-de la Garza, J.A., Quintero, J. and Aroca, G. (2017). Bioethanol production from *Agave lechuguilla* biomass pretreated by autohydrolysis. *Revista Mexicana de Ingeniería Química 16*, 467-476.

Painuly, J.P. (2001). Barriers to renewable energy penetration; a framework for analysis. *Renewable Energy 24*, 73-89.

Proskurina, S., Heinimö, J., Schipfer, F. and Vakkilainena, E. (2017). Biomass for industrial applications: The role of torrefaction. *Renewable Energy 111*, 265-274.

Sanchez-Herrera, D., Sanchez, O., Houbron, E., Rustrian, R., Toledano, T., Tapia-Tussell, R., and Alzate-Gaviria, L. (2018). Biomethane potential from sugarcane straw in Veracruz, Mexico: Combined liquid hot water pretreatment and enzymatic or biological hydrolysis. *Revista Mexicana de Ingeniería Química 17*, 1105-1120.

Trejo, E., Martell, F., Micheloud, O., Teng, L., Llamas, A. and Montesinos-Castellanos, A. (2012). A novel stimation of electrical and cooling losses in electric arc furnaces. *Energy 42*, 446-456.

Zuru, A.A., Dangoggo S.M., Birnin-Yauri, U.A. and Tambuwal, A.D. (2004). Adoption of thermogravimetric kinetic models for kinetic analysis of biogas production. *Renewable Energy 29*, 97-107.